Evolution of Shear-Induced Melting in a Dusty Plasma

Yan Feng,[*] J. Goree, and Bin Liu

Department of Physics and Astronomy, The University of Iowa, Iowa City, Iowa 52242
(Received 9 October 2009; published 22 April 2010)

The spatiotemporal development of melting is studied experimentally in a 2D dusty plasma suspension. Starting with an ordered lattice, and then suddenly applying localized shear, a pair of counterpropagating flow regions develop. A transition between two melting stages is observed before a steady state is reached. Melting spreads with a front that propagates at the transverse sound speed. Unexpectedly, coherent longitudinal waves are excited in the flow region.

Applying shear can induce melting [1–5]. Experiments have been reported in soft materials: colloidal suspensions [6,7], two-dimensional (2D) electron crystals with magnetic field [8], foams [9], polymer glasses [10] and dusty (complex) plasmas [11]. Most of these studies were done with a steady application of shear.

If shear were instead applied suddenly, one could investigate the spatiotemporal development of shear-induced melting. However, there have been no such experiments reported in any physical system to our knowledge.

In addition to melting, another result of sudden application of shear is wave excitation. When strong shear is applied to a 2D crystal lattice, plastic deformation occurs, and this can cause melting [11]. When the applied shear is weaker and deformation is elastic, transverse waves (phonons) propagate through the lattice [12]. Another type of wave is longitudinal. To our knowledge, at least within the literature for dusty plasmas, there have been no reports of the excitation of coherent *longitudinal* waves due to the application of *shear* in either the elastic or plastic regimes.

Here we seek answers to three questions. First, can coherent longitudinal waves be generated by applying shear? Second, when shear is applied suddenly, and melting occurs, what is the spatiotemporal development? Third, is there a melting front, and how does it spread?

Physical systems that allow motion essentially on a 2D plane include a Wigner lattice of electrons on a liquid-He surface [8], ions confined in a Penning trap [13], colloidal suspensions [14], granular fluids [15], vortex arrays in the mixed state of type-II superconductors [16], and dusty plasmas levitated in a single layer [17,18].

Melting of 2D systems has a different mechanism than for 3D systems [14]; it is sometimes termed an order-disorder transition [19]. Order and disorder are characterized by measures of structure. For example, the local sixfold bond-orientational order $|\phi_6|$ [2,3,20] measures local order, while global order can be characterized by the abundance of defects [17,19], which are nonhexagonal Wigner-Seitz cells in Voronoi diagrams [3,17].

Dusty plasma is partially ionized gas containing micron-size particles of solid matter [17]. Dusty plasmas allow atomistic scale observation of dynamics by tracking parti-

cles with video microscopy, and they also allow laser manipulation of particles [17]. We will exploit these capabilities to observe at an atomistic scale, with both spatial and temporal resolution, the sudden onset of shear-induced melting. In most previous dusty plasma experiments, melting was studied under steady-state conditions (by changing plasma parameters [21–23], varying particle number [24], and laser manipulation [11,25]). The temporal development of melting has received less study, and experiments that have been reported [17,26] relied on mechanisms other than shear-induced melting.

Particles have an electrical charge Q and are electrically confined in a single horizontal layer where they self-organize with a structure analogous to a crystalline solid or a liquid [17]. Coulomb repulsion is shielded with a screening length λ_D [27]. Dusty plasmas are driven-dissipative systems [17,28], with frictional drag on the rarefied gas at a damping rate ν_f [29]. The collective oscillation of particles can be characterized by the nominal 2D dust plasma frequency ω_{pd} [30].

For a dusty plasma suspension, shear must be applied differently than for most substances (e.g., colloidal suspensions [7]) because the suspension does not contact a container. We apply shear internally within our sample, using laser radiation pressure [11,20].

Using the apparatus of [28], an argon plasma was generated in the vacuum chamber at 15.5 mTorr, powered by 13.56 MHz radio-frequency voltages at 184 V peak to peak. The particles were polymer microspheres with a diameter 8.1 μm and a gas damping rate $\nu_f = 2.7$ s^{-1} [29].

The particles were suspended in a single layer. Before applying shear they self-organized in a triangular lattice with sixfold symmetry [17]. Particle motion was essentially 2D, with negligible out-of-plane displacements and no buckling of the particle layer. The suspension had a diameter ≈ 52 mm and contained $>11\,000$ particles. About 2800 particles were in the analyzed region, (24.7×20.4) mm^2. The particle spacing was characterized by a Wigner-Seitz radius [30] $a = 0.25$ mm.

To apply shear stress with a sudden onset, we used laser radiation pressure, which applies forces internally within the sample [11]. The power of a pair of 532-nm laser beams

was increased within 40 ms to a constant level. A different
constant level was chosen for each of our four runs, varying
from 0.57 to 1.90 W per beam, as measured inside the
chamber. The beams pointed oppositely in the $\pm x$ direc-
tions and struck the suspension at a 6° downward angle.
Their width and separation were $\Delta Y_l \approx 0.2$ mm and $L =$
4.7 mm, respectively. To apply shear across the entire
suspension width, the beams were rastered across the full
suspension (at a frequency high enough, 200 Hz, to avoid
exciting coherent waves at the rastering frequency [25]).

Using a top-view camera, we recorded videos for a
duration of 14 s (including 5 s before applying shear).
While applying shear, particles flowed out of the camera's
field of view (FOV); they circulated around the suspen-
sion's perimeter and then reentered the FOV [11]. Between
runs we turned laser manipulation off for ≈ 20 min, so
that the suspension had enough time to cool, solidify and
anneal [17]. Then we calculated particle positions and
velocities in each video frame [17].

Using the wave-spectra analysis method for particle
random motion in an ordered lattice [31], we found these
parameters for our dusty plasma: $\omega_{pd} = 72.6$ s^{-1}, $Q/e =$
$-(8700 \pm 900)$, $\lambda_D = (0.33 \pm 0.07)$ mm. The same
method also yielded the transverse and longitudinal
sound speeds, $C_t = (4.0 \pm 0.4)$ mm/s and $C_l = (15.0 \pm$
1.5) mm/s, respectively. When coherent waves are ob-
served experimentally, they can be identified as transverse
or longitudinal waves by their speed and by the direction
v_x or v_y of particle motion.

The experiment was designed to have symmetry with an
ignorable coordinate x. We average some quantities over x,
as denoted by $\langle \cdots \rangle_x$ (averaging with cloud-in-cell weight-
ing with a bin width of the lattice constant, 1.9a). The
kinetic energy (KE) is averaged over both x and y for the
full analyzed region, as denoted by $\langle \cdots \rangle_{xy}$. We calculate
KE = KE$_x$ + KE$_y$, where KE$_x$ = $m\langle v_x^2 \rangle_{xy}/2$, and simi-
larly for KE$_y$. Although this definition includes the energy
of directed flow as well as random motion, we will report
the values in temperature units (K), to allow comparison to
other experiments.

Results in Figs. 1(a) and 1(b) show the development of
KE and the flow velocity after we suddenly applied shear
stress. The KE increases dramatically, by about 2 orders of
magnitude, Fig. 1(a). Melting occurs for laser powers
above a threshold ≈ 0.4 W. The flow pattern, Fig. 1(b),
broadens until reaching a steady state at ≈ 1 s, when the
full width at half maximum (FWHM) of the velocity
profile is $\Delta Y_f = 1.2$ mm, which we will refer to as the
flow regions. This width ΔY_f is determined by a combi-
nation of shear stress applied by the laser, gas friction, and
shear viscosity of the suspension [11]. The KE is greater
for velocities in the x direction than in the y direction
because shear was applied in the x direction ($\approx 53\%$ of
KE$_x$ is due to directed flow in the steady state). Scale
lengths in the flow are ordered as $\Delta Y_l \approx a < \Delta Y_f < L$.
The flow is laminar, with a Reynolds number $\ll 10^2$ [11].

In the flow region, the kinetic temperature (estimated from
v_y) is high, with $\Gamma \approx 20$; this is well beyond the predicted
melting point $\Gamma = 160$ [32].

To answer our first question, we observe coherent *lon-
gitudinal* waves propagating away from the flow region.
This result might be surprising because the energy input
was purely shear. These longitudinal waves are revealed in
Fig. 1(c) by wave fronts with a slope corresponding to the
longitudinal sound speed, C_l. The wave fronts emerge from
the flow region, suggesting that the longitudinal waves
were generated there. These wave fronts repeat, indicating
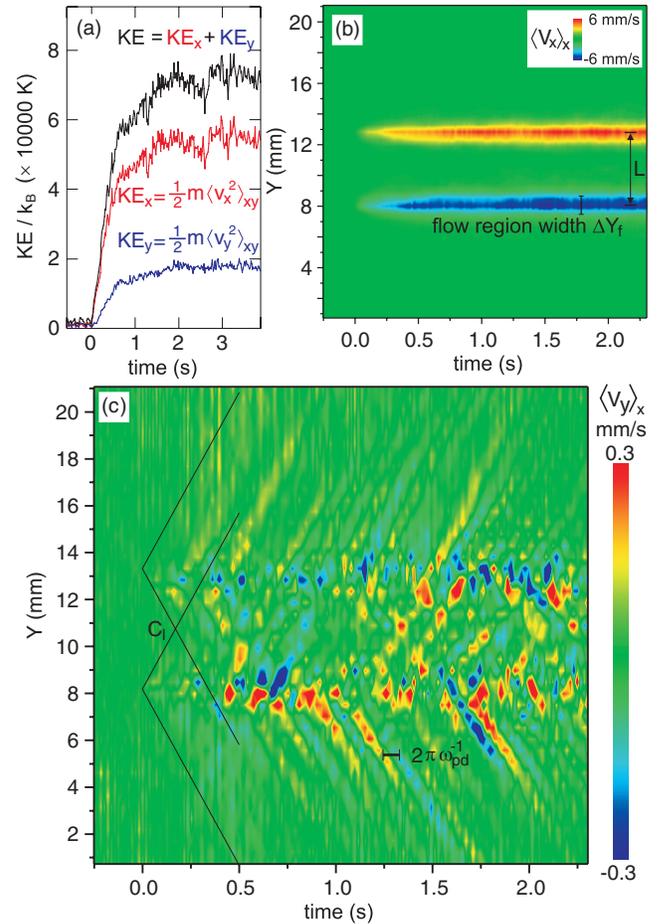the waves are coherent, not random.

FIG. 1 (color online). (a) Time series of the average kinetic
energy (KE). Shear was applied suddenly by applying 0.95 W
of laser power starting at $t = 0$. The KE rose about 2 orders
of magnitude until a steady state was reached at ≈ 1 s.
(b) Spatiotemporal evolution of the flow velocity $\langle v_x \rangle_x$. Two
counterpropagating flow regions broaden to a width ΔY_f (de-
fined as FWHM of the velocity profile). Length scales, including
the thickness ΔY_l and spacing L of the laser sheets, are ordered
as $\Delta Y_l \approx a < \Delta Y_f < L$. (c) Coherent longitudinal waves, gen-
erated near the flow region and propagating outward. This is
revealed by the repeated pattern of wave fronts in this plot of
$\langle v_y \rangle_x$. For comparison, the longitudinal sound speed C_l is in-
dicated by the straight lines. The observed wave period is
$\approx 4\pi\omega_{pd}^{-1}$.

The coherent longitudinal waves in Fig. 1(c) have a period $\approx 4\pi\omega_{pd}^{-1}$. This is the almost the same as the period where the dispersion relations of longitudinal and transverse waves cross [33]. This observation suggests that the coherent longitudinal waves we observe could be explained by scattering from transverse waves.

Energy is carried into the surrounding lattice by these coherent longitudinal waves. We will consider the speed of these waves below, when explaining sudden shear-induced melting.

To answer our second question, we find that after sudden application of shear, melting occurs in two steps. Examining Fig. 2(a), we can see that defects initially proliferate at a higher rate, then soon after at a slower rate, with a distinctive transition between. We term these "melting stages" 1 and 2. Afterwards, at a long time, there is of course a steady state. We confirmed that the transition is ubiquitous: it occurs for all four laser powers we tested, and also in other suspensions with various values of the particle spacing.

Our experiment provides both spatial and temporal resolution, which we can exploit to investigate the cause of the transition between the two melting stages. We are motivated by Fig. 1(b) to analyze time series separately in two spatial portions: inside and outside the flow regions. This yields the time series in Fig. 2(b), where the quantity plotted is the defect number fraction, calculated by dividing the number of defects by the number of particles.

Figure 2(b) reveals that defects proliferate in different places at different times. In melting stage 1, they proliferate mainly inside the flow regions until saturating at $t = 0.16$ s. Importantly, this is the same time as the transition in Fig. 2(a). Only afterwards do defects spread widely outside the flow region, as seen in the bottom curve in Fig. 2(b). Thus, the transition in the phase diagram arises from the different timing of when defects appear in the two different regions: first inside the flow region until defects saturate there, and then outside.

We can quantify the physical time scales for the two melting stages. Candidate time scales include ω_{pd}^{-1}, which characterizes mutual particle motion due to interparticle electric fields, and ν_f^{-1} due to gas friction. Initially, when velocities are low, we expect friction to be small, leading us to consider ω_{pd}^{-1} as the time scale for melting stage 1. We find that melting stage 1 has a duration on the order of $10\omega_{pd}^{-1}$, no matter how much shear is applied, as shown in Fig. 2(a). Later, as the KE increases, Fig. 2(b), dissipation by gas friction grows until it balances the energy input from the laser, yielding a steady state. The role of friction in limiting the spread of melting is suggested by noting that the duration of melting stage 2 is $\approx 1.5\nu_f^{-1}$.

To answer the third question, we find that there is a distinctive melting front, and it propagates at about the transverse sound speed, C_t. This is seen in Fig. 3, where the colored contours show how disorder spreads with time. We also draw lines with a slope corresponding to C_t; comparing these to the melting front, we see that they coincide. Thus, the melting front propagates at about C_t, not the much faster C_l. We verified this result using three different measures of structure. These include the local sixfold bond-orientational order $|\phi_6|$ [2,3,20] (as shown in Fig. 3), defect number fraction, and height of the first peak of the local pair correlation function.

Before this experiment, it was not obvious whether the melting front should spread at a rate corresponding to C_t, C_l, or thermal conduction. Thermal motion can be decomposed into incoherent waves that include both transverse and longitudinal modes. Coherent waves are also present, including the surprising longitudinal modes we found propagating away from the flow region. Thermal conduc-
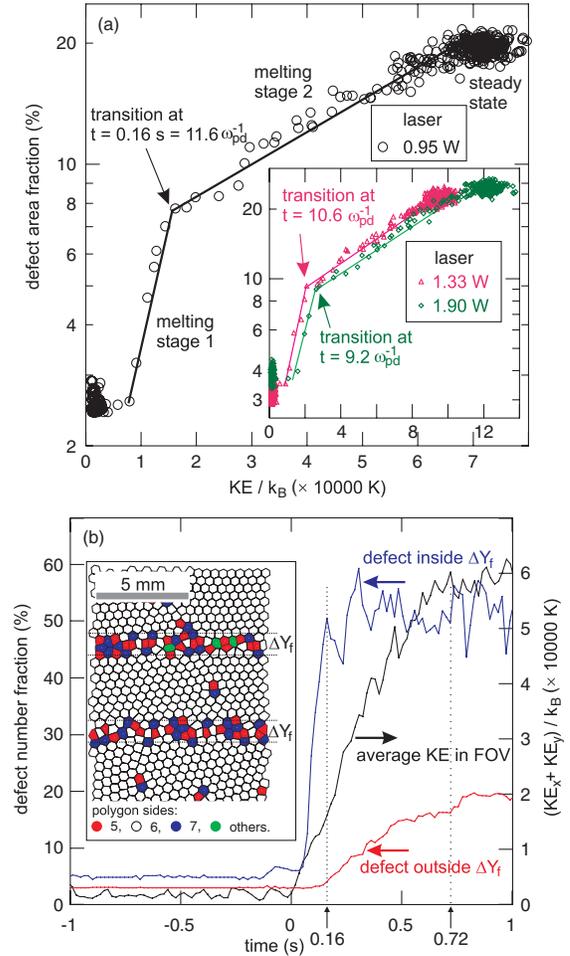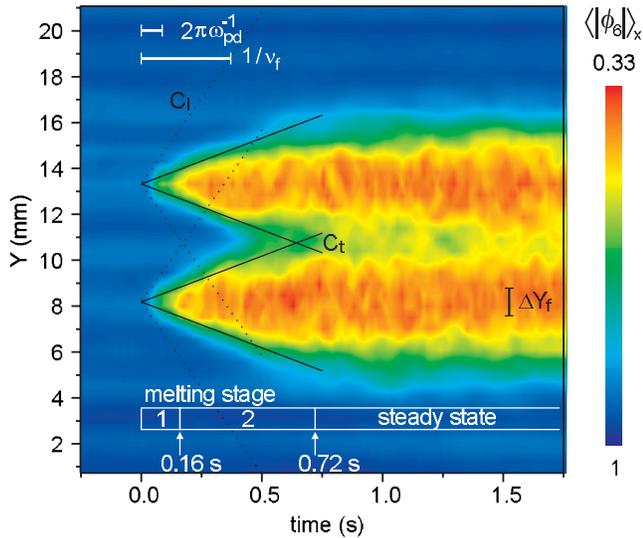

FIG. 2 (color online).   (a) Phase diagram, showing the proliferation of defects as the KE increases, recorded at 0.018 s intervals, for three laser powers. A transition between two stages is revealed. The quantity plotted is the defect area fraction; this measure of structure is the area of a Voronoi diagram that is occupied by defects [17], divided by the total area. (b) Time series for KE and defects, counted separately inside and outside the flow regions of width ΔY_f. The timing indicates that defects proliferate outside only after they saturate inside the flow regions. (The inset shows about 1/4 of the Voronoi diagram, for the run at 0.95 W at $t = 0.16$ s.)

FIG. 3 (color online). Spatiotemporal evolution of orientational order, $|\phi_6|$, which is defined to have a maximum of unity for a perfectly crystalline region [2,3,20]. Lines are drawn with the slopes C_t and C_l, starting at $t = 0$. The transverse sound speed, C_t, coincides with the melting front propagation. The resolution of our data along the Y axis is $1.9a$.

tion due to temperature gradients [34–36] would also lead to a spreading of energy as time passes.

To determine whether the flow of energy is in the form of waves or thermal conduction [34–36], we varied the laser power, which will vary the gradients. Linear waves propagate at the same speed, regardless of their amplitude, but energy spreads by thermal conduction more rapidly if the gradients are larger. We found that the melting front propagated at nearly C_t for all four laser powers we tested. Thus, we dismiss thermal conduction as the main mechanism for the propagation of energy that results in the melting front.

Our result that the melting front propagates at about C_t suggests that the propagation of transverse waves is the mechanism for transferring the energy required for melting in our experiment. Transverse waves, which were excited when shear was first applied, propagate outward carrying energy that can create defects. As this wave front travels, it loses energy by creating disorder and by gas friction. Eventually, after traveling about 3 mm, the outward traveling wave loses so much energy that it can no longer generate more defects, and the steady state is reached. It is possible that in other systems, with greater applied shear, the generated coherent longitudinal waves might be strong enough to melt a solid lattice, so that the melting front would propagate at C_l.

In summary, we found that coherent longitudinal waves are excited in this shear-induced melting system. Applying shear suddenly led to melting in two stages separated by a distinctive transition. After defects saturated within narrow flow regions, they spread wider with a melting front that propagates at about C_t

*yan-feng@uiowa.edu

[1] S. Ramaswamy and S. R. Renn, Phys. Rev. Lett. **56**, 945 (1986).
[2] T. Weider, M. A. Glaser, H. J. M. Hanley, and N. A. Clark, Phys. Rev. B **47**, 5622 (1993).
[3] J. Delhommelle, Phys. Rev. B **69**, 144117 (2004).
[4] S. Butler and P. Harrowell, Nature (London) **415**, 1008 (2002).
[5] R. Messina and H. Löwen, Phys. Rev. E **73**, 011405 (2006).
[6] B. J. Ackerson and N. A. Clark, Phys. Rev. Lett. **46**, 123 (1981).
[7] C. Eisenmann, C. Kim, J. Mattsson, and D. A. Weitz, Phys. Rev. Lett. **104**, 035502 (2010).
[8] L. Wilen and R. Giannetta, Jpn. J. Appl. Phys., Suppl. **26-3**, 2105 (1987).
[9] A. D. Gopal and D. J. Durian, J. Colloid Interface Sci. **213**, 169 (1999).
[10] D. A. Weitz, Science **323**, 214 (2009).
[11] V. Nosenko and J. Goree, Phys. Rev. Lett. **93**, 155004 (2004).
[12] S. Nunomura, D. Samsonov, and J. Goree, Phys. Rev. Lett. **84**, 5141 (2000).
[13] T. B. Mitchell et al., Phys. Plasmas **6**, 1751 (1999).
[14] C. A. Murray, W. O. Sprenger, and R. A. Wenk, Phys. Rev. B **42**, 688 (1990).
[15] P. M. Reis, R. A. Ingale, and M. D. Shattuck, Phys. Rev. Lett. **96**, 258001 (2006).
[16] P. L. Gammel et al., Phys. Rev. Lett. **59**, 2592 (1987).
[17] Y. Feng, J. Goree, and B. Liu, Phys. Rev. Lett. **100**, 205007 (2008).
[18] S. Ratynskaia et al., Phys. Rev. Lett. **96**, 105010 (2006).
[19] C. Reichhardt and C. J. Olson Reichhardt, Phys. Rev. E **77**, 041401 (2008).
[20] W.-Y. Woon and L. I, Phys. Rev. Lett. **92**, 065003 (2004).
[21] H. M. Thomas and G. E. Morfill, Nature (London) **379**, 806 (1996).
[22] A. Melzer, A. Homann, and A. Piel, Phys. Rev. E **53**, 2757 (1996).
[23] T. E. Sheridan, Phys. Plasmas **15**, 103702 (2008).
[24] A. V. Ivlev, U. Konopka, G. Morfill, and G. Joyce, Phys. Rev. E **68**, 026405 (2003).
[25] V. Nosenko, J. Goree, and A. Piel, Phys. Plasmas **13**, 032106 (2006).
[26] D. Samsonov et al., Phys. Rev. Lett. **92**, 255004 (2004).
[27] U. Konopka, G. E. Morfill, and L. Ratke, Phys. Rev. Lett. **84**, 891 (2000).
[28] B. Liu and J. Goree, Phys. Rev. Lett. **100**, 055003 (2008).
[29] B. Liu, J. Goree, V. Nosenko, and L. Boufendi, Phys. Plasmas **10**, 9 (2003).
[30] G. J. Kalman, P. Hartmann, Z. Donkó, and M. Rosenberg, Phys. Rev. Lett. **92**, 065001 (2004).
[31] S. Nunomura et al., Phys. Rev. Lett. **89**, 035001 (2002).
[32] P. Hartmann et al., Phys. Rev. E **72**, 026409 (2005).
[33] S. Nunomura, S. Zhdanov, D. Samsonov, and G. Morfill, Phys. Rev. Lett. **94**, 045001 (2005).
[34] V. E. Fortov et al., Phys. Rev. E **75**, 026403 (2007).
[35] V. Nosenko et al., Phys. Rev. Lett. **100**, 025003 (2008).
[36] L.-J. Hou and A. Piel, J. Phys. A **42**, 214025 (2009).